Electronic Supplementary Information for Dalton Transactions

3D-Transition Metal Mono-Substituted Keggin Polyoxotungstate with an Antenna Molecule: Synthesis, Structure and Characterization

Hongsheng Liu[a], Carlos J. Gómez-García[b], Jun Peng*[a], Jingquan Sha[a], Yangguang Li[a], Yechao Yan[a]

[a] *Key Laboratory of Polyoxometalate Science of Ministry of Education Faculty of Chemistry, Northeast Normal University, Changchun, Jilin, 130024, P. R. China*

[b] *Instituto de Ciencia Molecular. ICMol. Universitat de Valencia. Pol La Coma s/n 46980 Paterna. Spain*

Supplementary Materials

Thermogravimetric (TG) Analysis

Thermogravimetric analyses of compounds **1**, **2** and **3** were carried out in nitrogen atmosphere with a heating rate of 10 °C min^{-1} in the temperature range 42-1000 °C. The TG/DTA curves of compounds **1-3** are shown in Figure S10-S12, respectively. The TG curve of compound **1** shows three distinct stages of weight loss in the temperature range 42-680 °C. The first weight loss of 3.9 % in the temperature range 42–140 °C corresponds to the release of crystallization water and is in agreement with the calculated value of 3.79 %. The successive weight loss of the second step (12 %) from 220 °C to 550 °C is in good agreement with the loss of the six protonated Im molecules (calc. 12.26 %). As expected, the coordinated Im ligand is lost at a higher temperature in a third step from 570 to 680 ºC. In this third step the weight loss (3.6 %) is higher than the expected value for one Im molecule, indicating that the lost of the coordinated Im ligand is accompanied by the lost of some oxygen atoms leaving a residue of WO_3, NiO and SiO_2 of 80.5 %, is in good agreement with the calculated value of 80.59 %. The DTA curve reveals two endothermic peaks at 66 °C and 288 °C which correspond to the loss of lattice water and the protonated Im molecules,

respectively. An additional exothermic peak at 631 °C corresponds to the oxidation of the coordinated Im ligand and/or to phase transformations of the residual inorganic oxides. As expected, the thermal behaviors of **2** and **3** are very similar to that of **1**.

The IR spectra (Figures S8-S9) and XRPD patterns (Figures S13-S14) of compounds **1** and **2** after heating to 550 °C have been performed, which strongly support the TG/DTA results, and suggest that the polyanions $[SiW_{11}O_{39}ZIm]^{6-}$ (Z = Ni^{II}, Mn^{II} and Co^{II}) are remarkably stable until 550 °C.

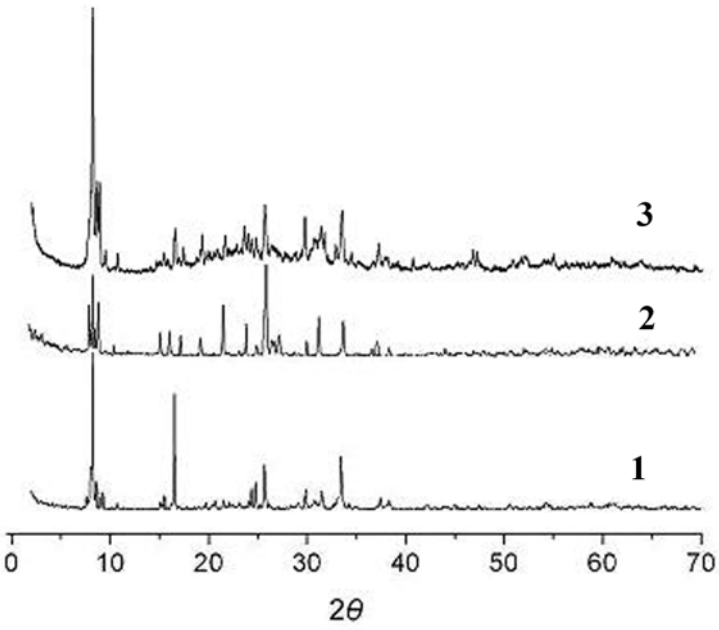

Figure S1. Experimental XRPD patterns of compound **1**, **2** and **3**.

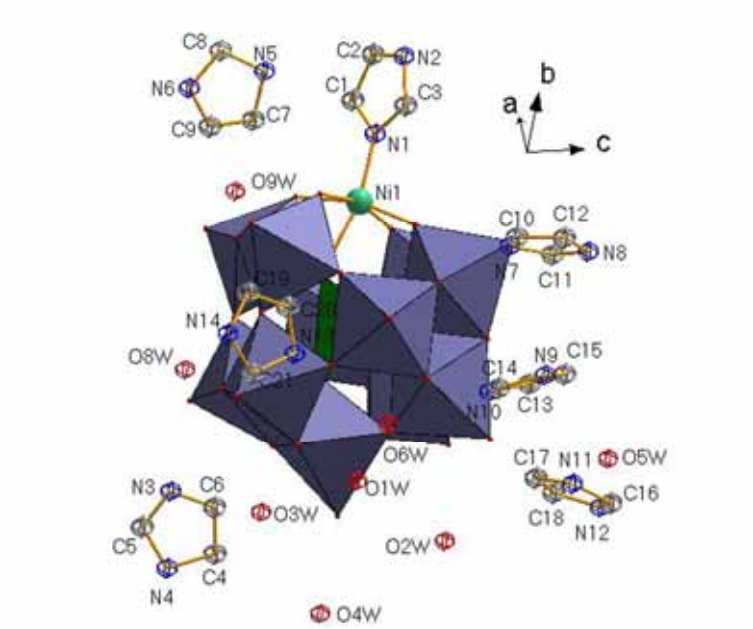

Figure S2. The molecular structure of compound **1**, showing the positions of polyanion and counteractions HIm^+, and H_2O molecules. Hydrogen atoms are omitted for clarity.

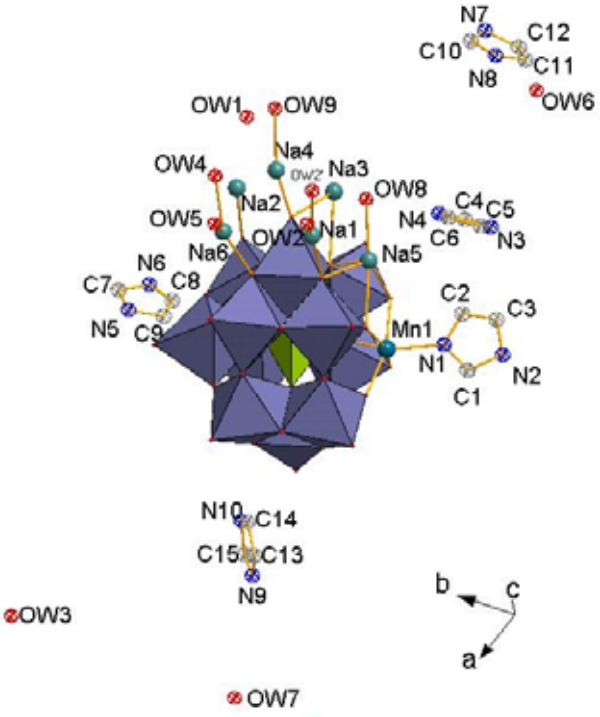

Figure S3. The molecular structure of compound **2**, showing the positions of polyanion and counteractions Na^+, and H_2O and Im molecules. Hydrogen atoms are omitted for clarity.

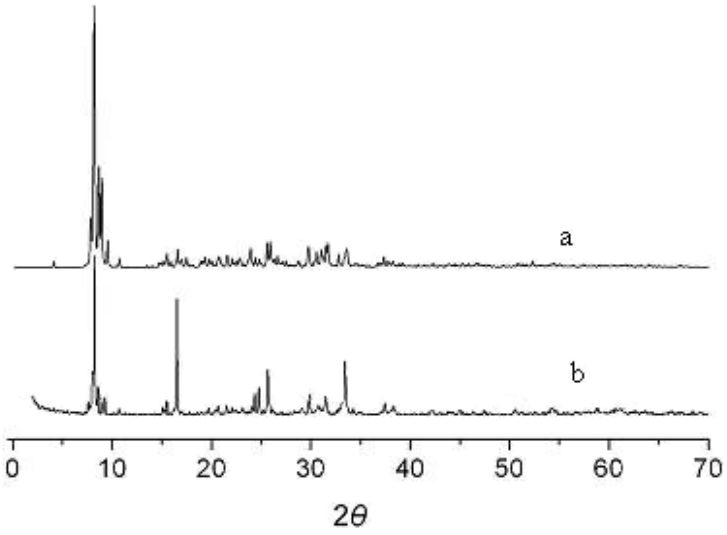

Figure S4. (a) Simulated and (b) experimental XRPD patterns of compound **1**.

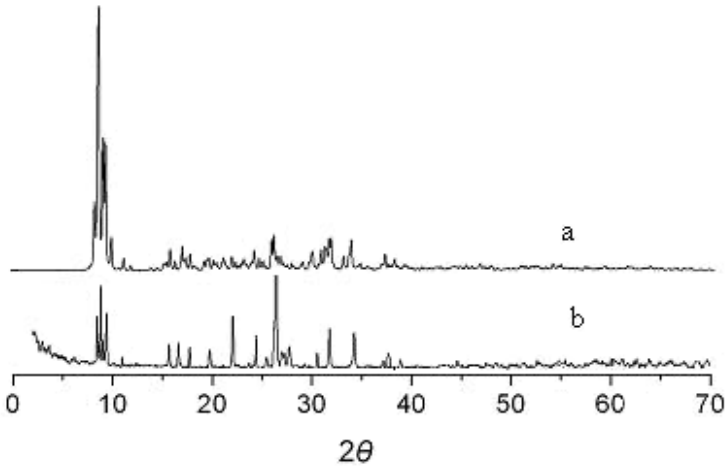

Figure S5. (a) Simulated and (b) experimental XRPD patterns of compound **2**.

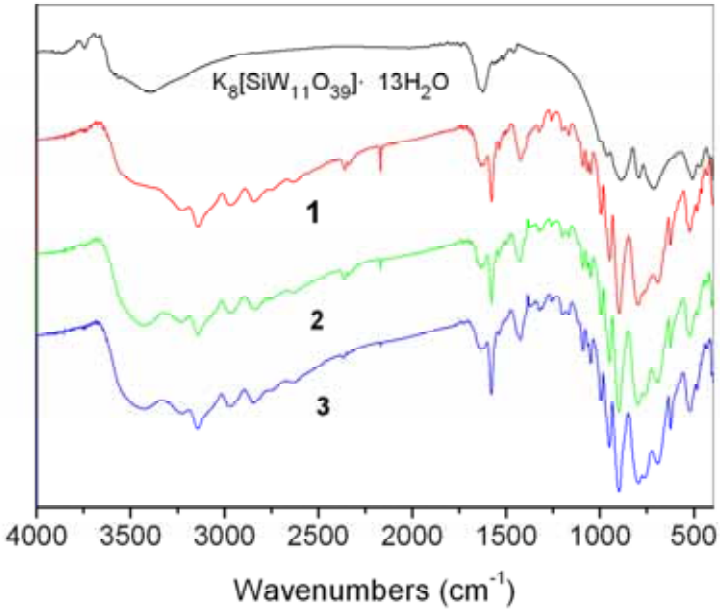

Figure S6. IR spectra for precursor, compounds **1**, **2** and **3**.

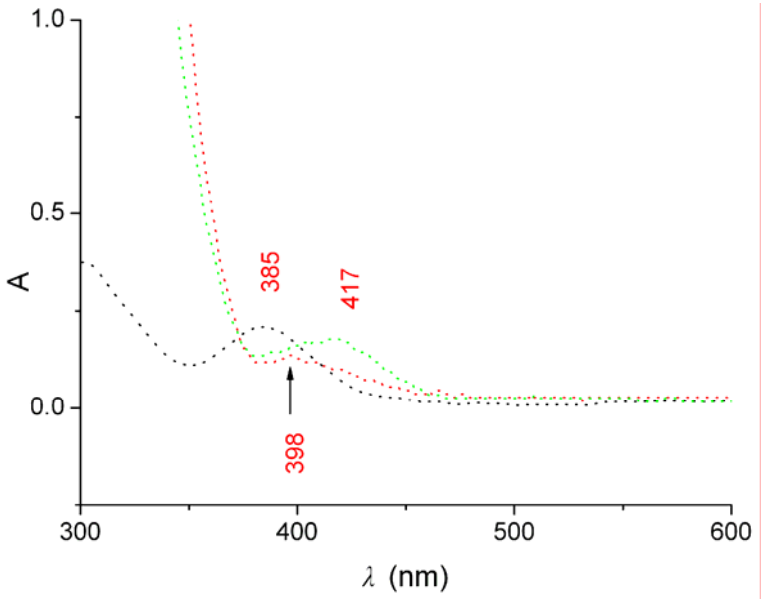

Figure S7. UV-vis spectra of the solution of compound **1** (green), $[SiW_{11}O_{39}Ni(H_2O)]^{6-}$ (red) and Ni complexes (black) in distilled water.

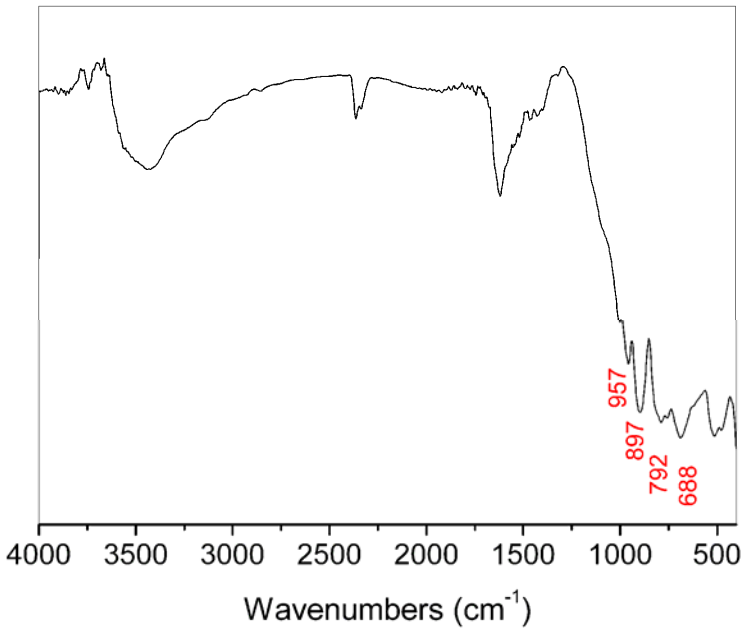

Figure S8. IR spectrum of compound **1** after heated to 550 ℃.

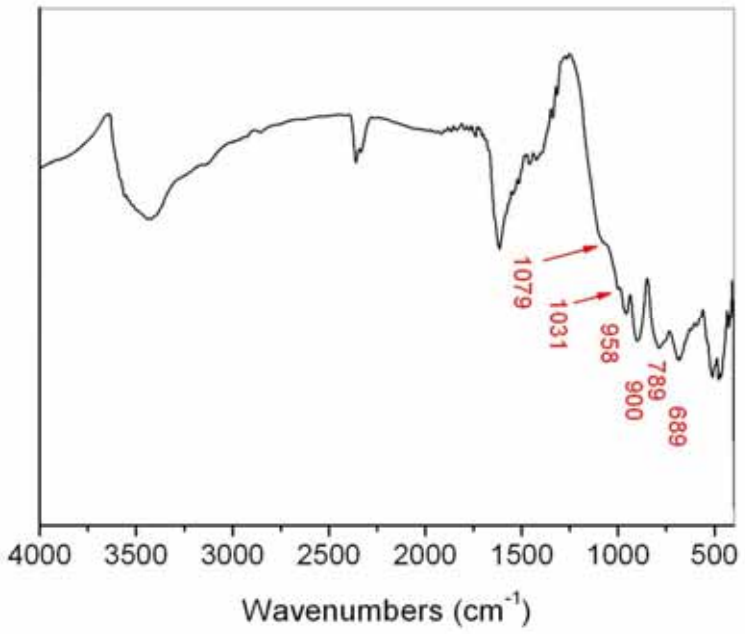

Figure S9. IR spectrum of compound **2** after heated to 550 ℃.

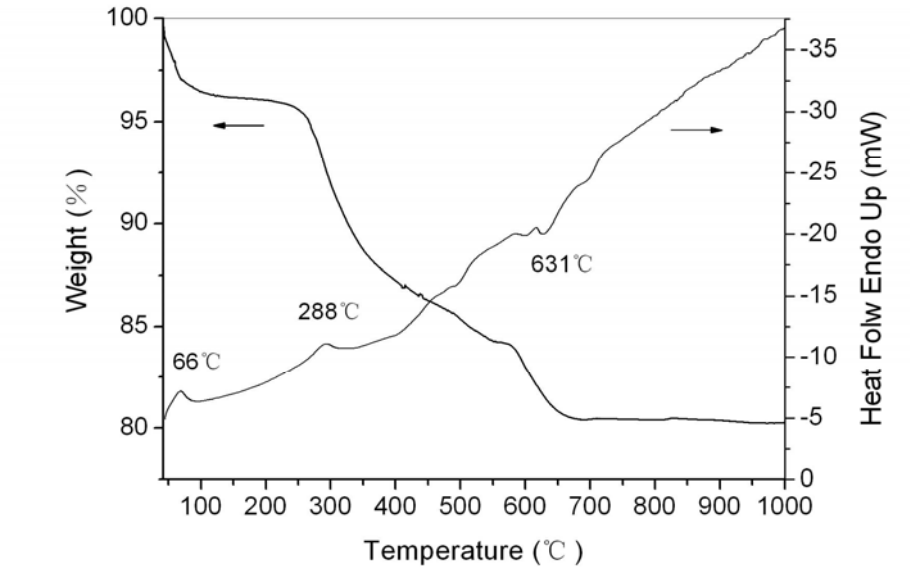

Figure S10. TG and DTA curves of compound **1**.

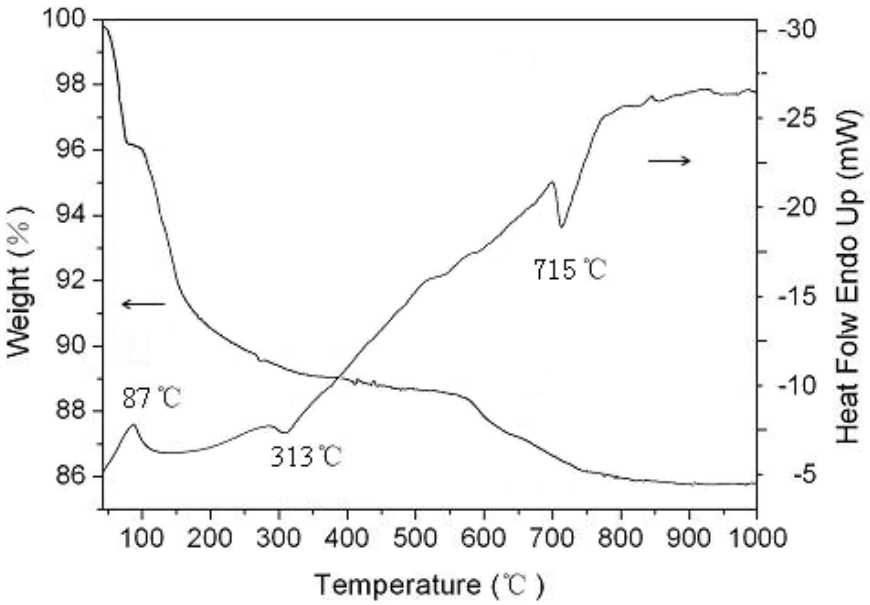

Figure S11. TG and DTA curves of compound **2**.

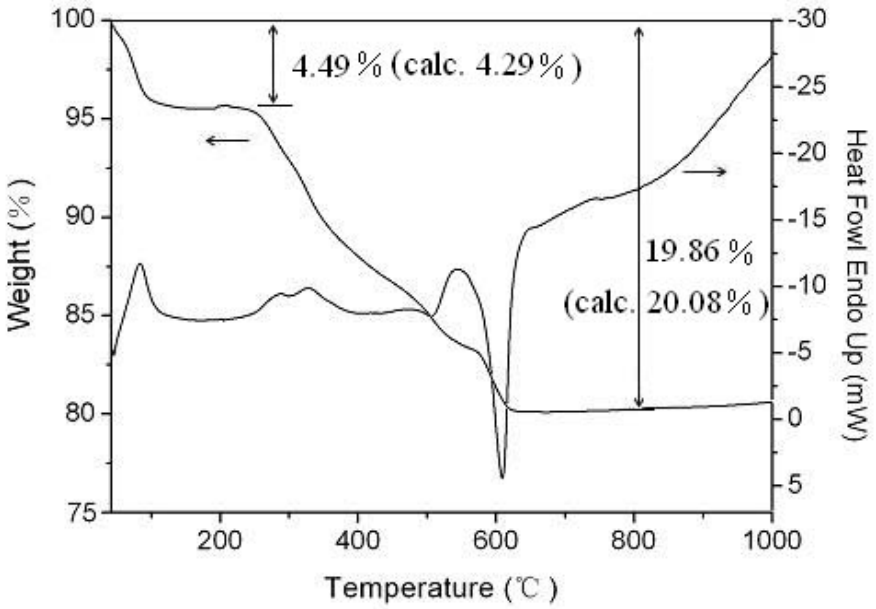

Figure S12. TG and DTA curves of compound **3**.

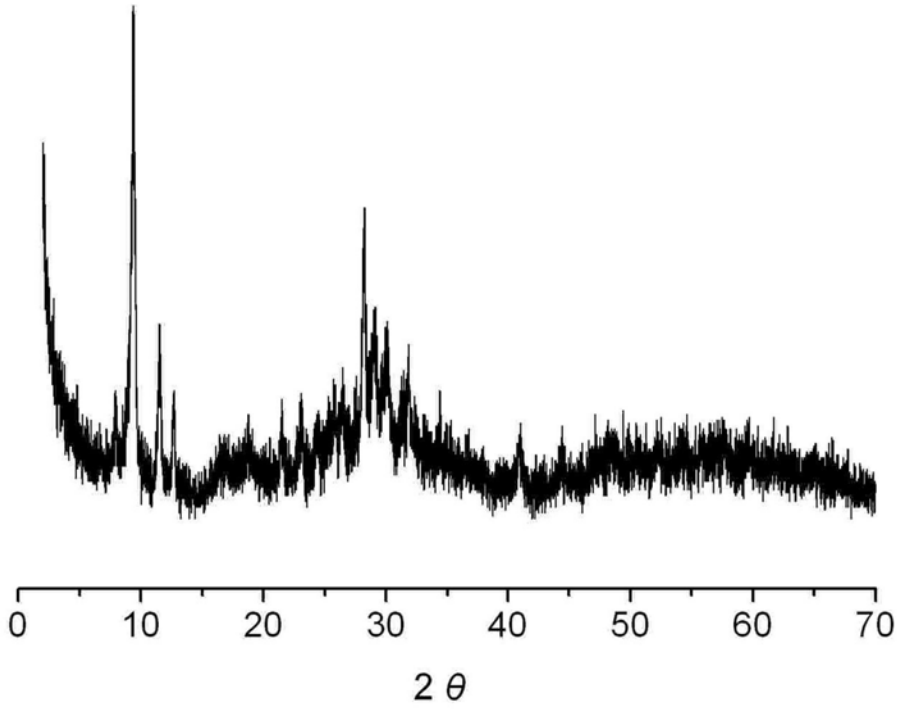

Figure S13. Experimental XRPD patterns of compound **1** after heated to 550 ℃.

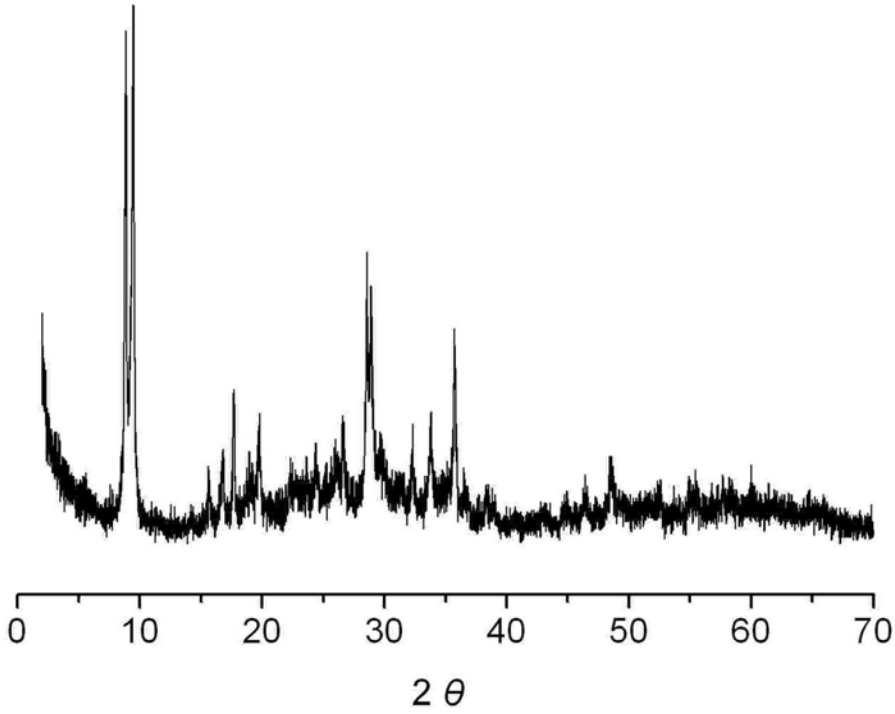

Figure S14. Experimental XRPD patterns of compound **2** after heated to 550 ℃.

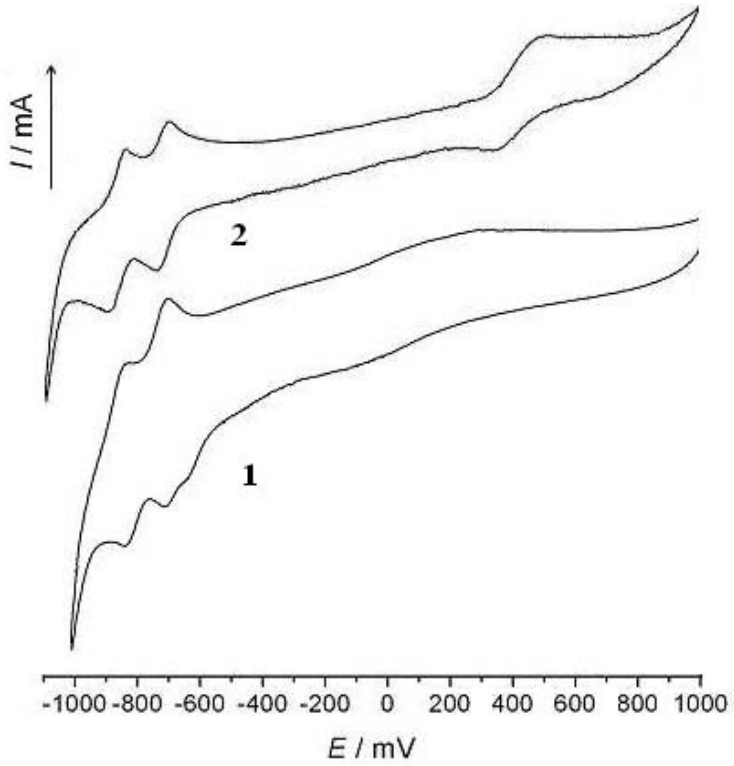

Figure S15. Cyclic voltammograms of compounds **1** and **2** (glassy-carbon working electrode, scan-rate 50mV s^{-1}, 0.5 M KAc/HAc buffer solution, pH 4.7).

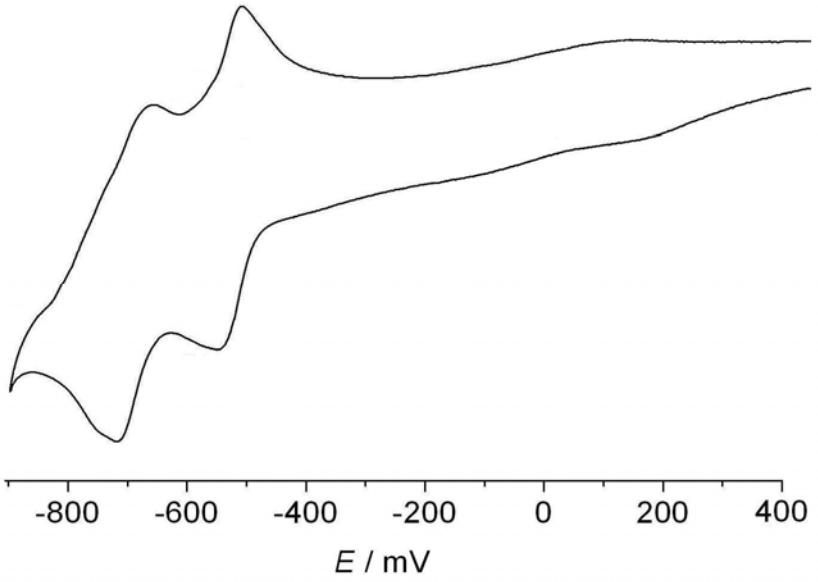

Figure S16. Cyclic voltammogram of compound $[SiW_{11}O_{39}Ni(H_2O)]^{6-}$ (glassy-carbon working electrode, scan-rate 50mV s^{-1}, 0.5 M KAc/HAc buffer solution, pH 4.7).

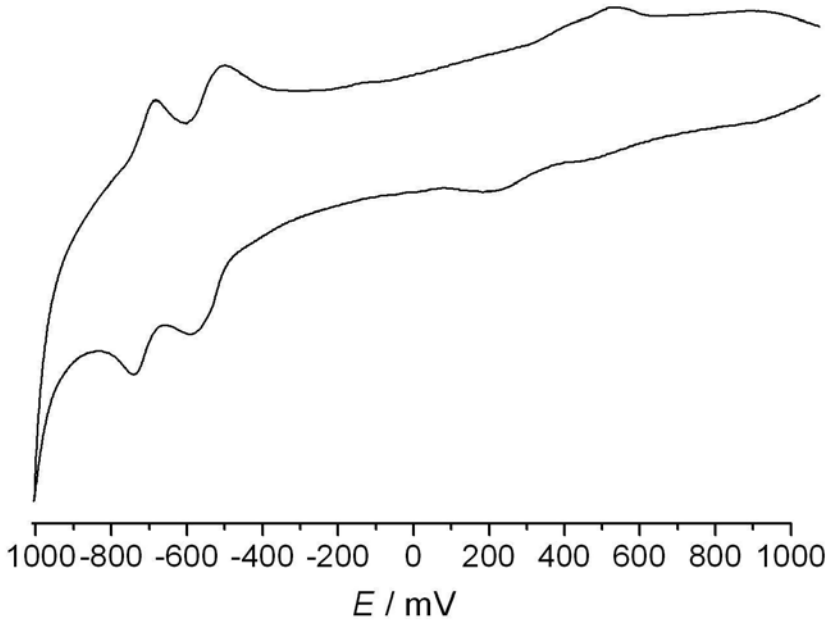

Figure S17. Cyclic voltammogram of compound $[SiW_{11}O_{39}Mn(H_2O)]^{6-}$ (glassy-carbon working electrode, scan-rate 50mV s^{-1}, 0.5 M KAc/HAc buffer solution, pH 4.7).

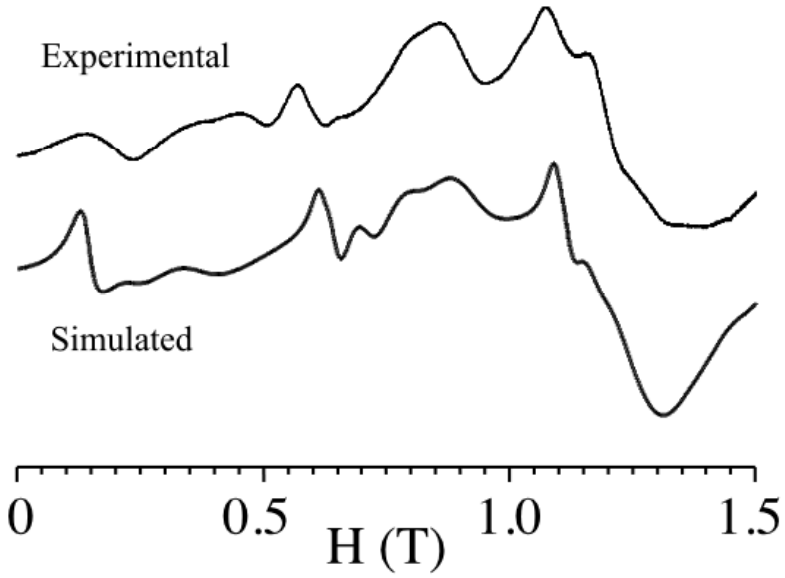

Figure S18. Experimental and simulated EPR spectra at 15 K of compound **2**.

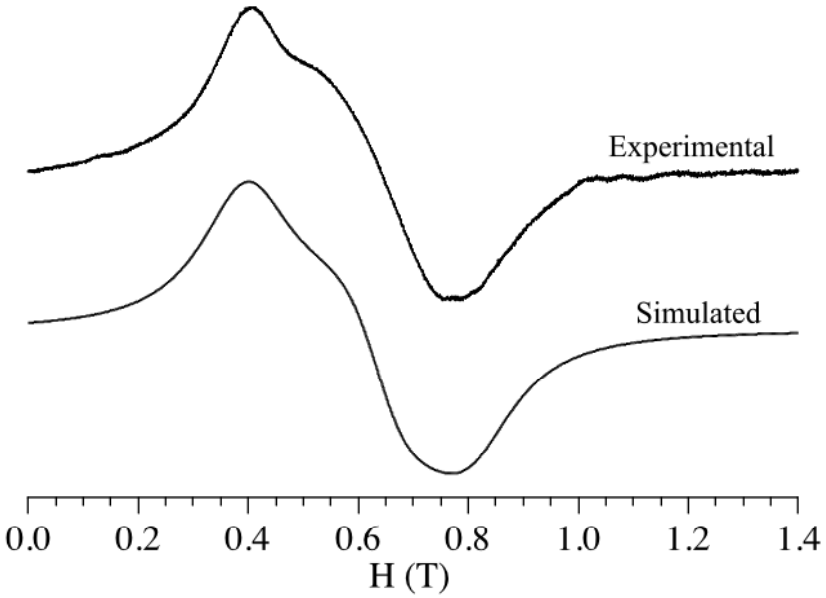

Figure S19. Experimental and simulated EPR spectra at 50 K of compound **3**.

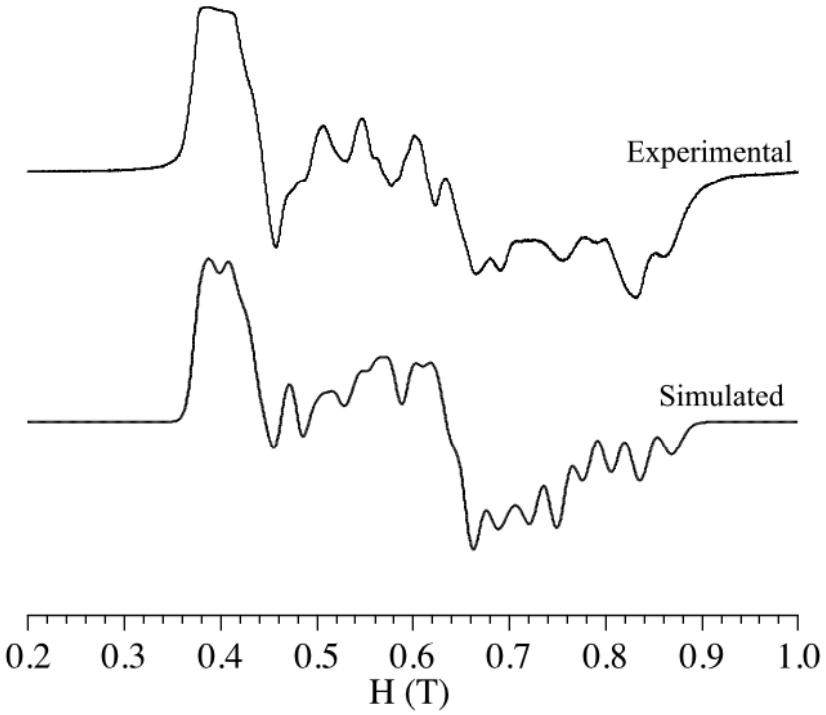

Figure S20. Experimental and simulated EPR spectra at 5 K of compound **3**.